Available online at www.sciencedirect.com
SCIENCE DIRECT®
Journal of Photochemistry and Photobiology A: Chemistry 164 (2004) 173–177
Journal of Photochemistry and Photobiology A:Chemistry
www.elsevier.com/locate/jphotochem

Preparation of a porous ITO electrode

Hong Lin [a,*], Tetsuro Jin [a], Andriy Dmytruk [b], Makoto Saito [c], Tetsuo Yazawa [d]

[a] *National Institute of Advanced Industrial Science and Technology, AIST Kansai, Ikeda, Osaka 563-8577, Japan*
[b] *Radiophysical Faculty, National Taras Shevchenko University of Kyiv, Kyiv 03122, Ukraine*
[c] *Specialty Chemicals Division, Chemicals Sector, Showa Denko K.K., Kawasaki, Kanagawa 210-0865, Japan*
[d] *Division of Material Engineering, Graduate School of Engineering, Himeji Institute of Technology, Himeji, Hyogo 671-2201, Japan*

Received 25 July 2003; received in revised form 20 December 2003; accepted 26 December 2003

Abstract

A porous electrode was prepared by introduction of indium tin oxide (ITO) into pores of a porous glass (PG) matrix with nano-size pores and thus forming an ITO/PG nanocomposite, using metallorganic chemical vapor deposition (MOCVD) method. The ITO/PG nanocomposite has through pores and a specific surface area of about 7.6×10^4 times larger than that of a plane transparent conductive glass. The porous electrode is suggested to be a good candidate of electrode used in photoelectric devices.
© 2004 Elsevier B.V. All rights reserved.

Keywords: Porous glass; Surface area; Electrode; ITO; Nanocomposite

1. Introduction

Transparent conductive film (TCF), usually indium tin oxide (ITO) or SnO_2, is indispensable as electrode used in modern photoelectric devices, such as liquid crystal/plasma/electroluminescence (EL) displays and solar cells. General requirement for TCF is high conductivity and high transparency in visible spectral region.

On the other hand, porous electrode may attract much interest in the field such as photoelectrochemistry, where transparency and electric conductivity of the electrode with large surface area are especially useful, since it can provide a large surface for supporting a large amount of functional materials. A dye-sensitized solar cell [1,2], which is formed by titania, dye, electrolyte, and a couple of TCF electrodes, is taken as an example here. Nano-porous titania with thickness of several micrometers and a large surface area is usually required to support a large amount of dye for obtaining a high light-to-energy conversion efficiency. There may be, however, limitation for further increase of the thickness of titania, because thick porous titania may increase its electric resistance, which in turn restrain electron transfer from titania to TCF electrode [3]. If the electrode used in dye-sensitized solar cell is nano-porous, the pores are expected not only to provide a huge surface, which can support a larger amount of functional materials of titania and dye, but also to decrease the thickness of titania layer, therefore to decrease its resistance as stated above. Consequently, the large surface formed by porous electrode may increase photoelectric device's function such as light-to-energy conversion efficiency drastically.

A flat dense ITO or SnO_2 film can be prepared on a glass substrate by MOCVD [4], spray [5], sputtering [6], oxygen ion beam assisted deposition [7] and so on, while deposition of conductive film on a silicate PG is a new idea to get transparent or translucent porous electrode. It is well known that PG is highlighted for its huge specific surface area and transparency in visible spectral region [8]. Generally, PG is made by acid-leaching of soluble borate phase in phase-separated alkaline borosilicate after heat-treatment, producing three-dimensional interconnecting pores through the essential silica skeleton. Specific surface area and pore size can be controlled by adjusting temperature and time of the heat-treatment process. Recently, PG has attracted a great attention as a host matrix to form nanocomposites [9–11]. In that case, its large surface could be effectively used to support large amount of functional materials. This merit has been widely utilized in photocatalysis field, where photocatalyst of titania anchored in the pores of PG [12] or porous alumina [13] showed enhanced photocatalytic activity. Dong and Gafney [14] deposited ITO on a PG substrate with pore diameter of 10 nm using spin-coating method. The ITO film they obtained is not porous and no evidence of ITO film in the pores is shown.

* Corresponding author.
E-mail address: hong-lin@tsinghua.edu.cn (H. Lin).

1010-6030/$ – see front matter © 2004 Elsevier B.V. All rights reserved.
doi:10.1016/j.jphotochem.2003.12.023

In the present study, we tried to prepare ITO film inside the pores of PG by MOCVD method. Considering later introduction of functional materials into the pores, PG with large pore diameter of about 50 nm was used, although it was slightly translucent white due to scattering of light. Sample preparation was carried out with or without evacuation from one side of PG plate. Evacuation from one side of PG plate is to introduce ITO into the pores of the porous matrix by pressure gradient, and thus to form a conductive nanocomposite, while keeping the system at atmospheric pressure (without evacuation) is to prepare ITO film just on the surface of PG plate.

2. Experimental

Figs. 1 and 2 show simple schematic diagrams of MOCVD experimental apparatuses, with and without evacuation from one side of the porous matrix. A porous silicate glass plate was used as a matrix for ITO deposition. It has a thickness of 1 mm and a mean pore diameter of about 50 nm, called PG50 in short. PG50 was fixed at the center of a glass chamber vertically by a couple of graphite screws, sealed with two pieces of graphite annular gaskets on the two sides of it (Fig. 1), or was put on the center of a glass chamber horizontally (Fig. 2). Indium dipivaloylmethanate ($In(DPM)_3$) and tin dipivaloylmethanate ($Sn(DPM)_2$) were used as precursors for preparing ITO film. A glass holder, filled with weighed precursors with molar ratio of Sn:In to be 10 mol%, was set in the glass chamber near the outer side of electric furnace. In the case of Fig. 1, the holder was set in chamber A, and chamber B was evacuated to 5.33×10^4 Pa (400 Torr), to make a pressure gradient between chamber A and B. The temperature at the center of the chamber was kept at 100 °C for more than 1 h to clean PG50 first, then heated to 300 °C, and at last kept at 500 °C for 1 h. Argon (Ar) was used for carrying vapor of precursors onto the porous matrix. The flow rate (R) of Ar was set at 5 ml/min. Oxygen (O_2) was used as a reactive gas to precursors. The flow rate of O_2 was varied from 5 to 20 ml/min. Ratio of the flow rates of the two gases was defined as ($r = R_{O_2}/R_{Ar}$). In the case of Fig. 2, PG50 was placed horizontally, and O_2 was introduced vertically to it. Therefore, O_2 would react with the precursors carried by Ar just at the upper side of PG50, which was supposed to be able to form a uniform film. The gases were introduced into the glass chamber after the temperature reached to 500 °C. The obtained samples were then heat-treated at 600 °C for 3 h in air atmosphere and for 6 h in N_2 atmosphere successively.

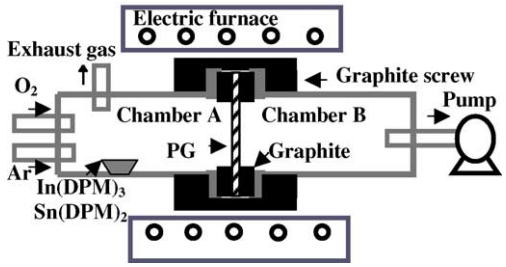

Fig. 1. Schematic diagram of MOCVD experimental apparatus with evacuation of glass chamber B to 5.33×10^4 Pa (400 Torr).

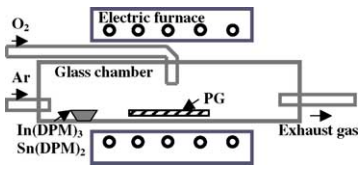

Fig. 2. Schematic diagram of MOCVD experimental apparatus at atmospheric pressure.

X-ray diffraction (XRD) measurements were carried out using an X-ray diffractometer (XRD-6000, Shimadzu, Japan) with Cu Kα radiation. The dc electrical resistances were recorded on an electrometer (Loresta–EP, MCP-T360, Mitsubishi Chemical Co., Japan) with four terminal probes at room temperature in air at drying condition. UV-Vis-NIR spectra were measured by a spectrophotometer (U-4000, Hitachi, Japan), with and without an integrating sphere. Microstructures were observed by a scanning electron microscope (SEM, JSM-5900LVS, Japan Electronic Datum Co.) and a field emission SEM (FESEM, S-4800, Hitachi, Japan). Qualitative analyses were carried out by using an energy dispersive X-ray system (EDX, Genesis 4000, EDAX, Japan). Pore size distributions were obtained with a mercury intrusion apparatus (Micromeritics Auto Pore IV, Shimadzu, Japan).

3. Results and discussion

When the temperature of the electric furnace with a length of 300 mm is set at 500 °C, the actual temperature near the outer side of the furnace decreases to about 100 °C suddenly. In case of filling asbestos around the glass chamber near the outer side of the furnace, the temperature there can be kept at about 200 °C. By thermogravimetry/differential thermal analysis (TG/DTA 6300, Seiko Instrument Inc., Japan), it is found that $In(DPM)_3$ decomposes from about 140 °C, and its weight does not change from about 270 °C. As for $Sn(DPM)_2$, the weight changes nearly from 70 to 410 °C. The precursors melted when the temperature of the glass chamber increased, and their vapors were carried by Ar gas to PG50.

The color of the obtained samples was blackish when ratio (r) of O_2 to Ar was 1, before heat-treatment. This may be attributed to carbonization of the organic component in the precursors not reacted completely, since O_2 is not enough in this case. The blackish color became lighter after heat-treatment at 600 °C for 3 h in air atmosphere due to the oxidation. When O_2 partial pressure increased (r = 2–4), samples prepared by evacuating from one side of PG50 (see Fig. 1) revealed a little milk-white, while samples prepared

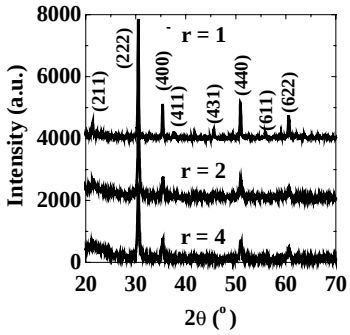

Fig. 3. XRD patterns of samples prepared by evacuating from one side of PG50, with different ratio (r) of O_2 to Ar.

at atmospheric pressure (see Fig. 2) showed no any color at all. No obvious change was observed in color for these samples with larger O_2 partial pressure after heat-treatment in air and N_2 atmosphere. The following data are generally for samples heat-treated in air and N_2 atmosphere, if there is no special statement.

3.1. ITO/PG nanocomposite prepared by evacuating from one side of PG50 (see Fig. 1)

Fig. 3 shows XRD patterns of the obtained samples prepared by evacuating from one side of PG50. The crystalline peaks of cubic-In_2O_3 (ASTM card no. 6-0416) are clearly seen in all the patterns. The peak intensity increases with the decrease of ratio (r) of O_2 to Ar, that is, O_2 partial pressure. SEM cross-section images show that lower O_2 partial pressure induces thicker ITO film. The thickness of the ITO film may determine the peak intensity of the XRD patterns.

Fig. 4 shows resistivity of the obtained samples versus the ratio (r) of O_2 to Ar. The resistivity of the samples increases with the increase of O_2 partial pressure. This may be ascribed to the decrease of oxygen defects, which are one of the most important conductive factors here. Kimura et al. [16] shows that carrier density may decrease with the increase of O_2 partial pressure since the generation of carrier made by oxygen defects should be restrained. Comparing

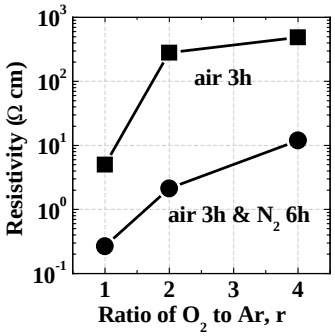

Fig. 4. Resistivity of samples prepared by evacuating from one side of PG50 vs. ratio (r) of O_2 to Ar.

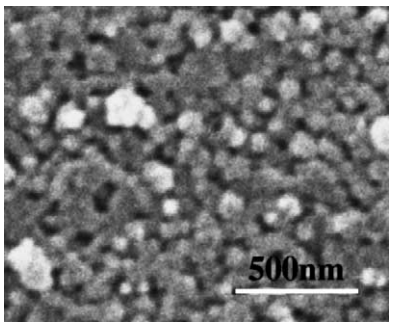

Fig. 5. SEM surface image of sample prepared by evacuating from one side of PG50 when $r = 4$. Bar: 500 nm.

heat-treatment in air, the resistivity of all the samples decreased more than 10 times after heat-treatment in N_2 atmosphere. This is attributed to the increase of oxygen defects generated in the inert gas atmosphere. The lowest resistivity of $10^{-1}\ \Omega$ cm is obtained when $r = 1$.

Fig. 5 shows typical SEM surface image of the sample prepared by evacuating from one side of PG50 when $r = 4$. The surface has rough morphology, formed by large interconnected particles with the particle diameter of several tens to hundred nanometers. Microstructure of the cross-section of the sample is shown in FESEM image in Fig. 6. Dark part in the image is silica skeleton of PG50, while bright part dispersed around the silica skeleton and on the upper surface of the PG plate are ITO film, according to EDX analysis. This image indicates that a nanocomposite of ITO/PG has been formed by the present preparation method. It also gives evidence that the layer of the ITO film formed on the upper surface of PG plate leaves the pores through. This may be attributed to the proper pressure gradient and preparation time.

Transparencies of all the samples were confirmed by observation under a fluorescent lamp and measured by a spectrophotometer, with and without an integrating sphere (IS), which is set for inspecting forward-scattered light from the sample. Fig. 7 shows UV-Vis-NIR spectra of the ITO/PG nanocomposite when $r = 2$, and that of an untreated PG50 as

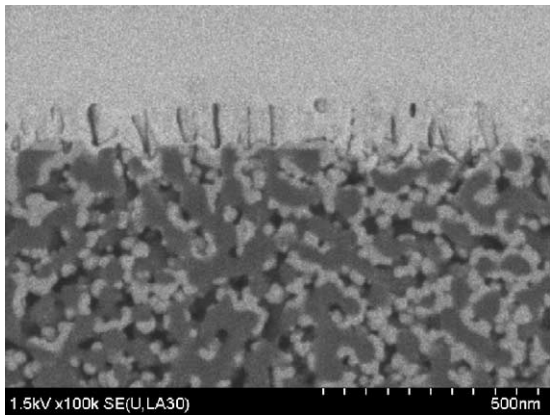

Fig. 6. FESEM cross-section image of sample prepared by evacuating from one side of PG50 when $r = 4$. The whole bar: 500 nm.

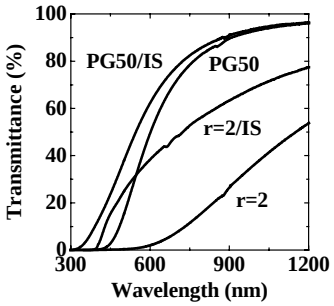

Fig. 7. UV-Vis-NIR spectra of sample prepared by evacuating from one side of PG50 when $r = 2$, and an untreated PG50 for reference, measured with and without an integrating sphere (IS).

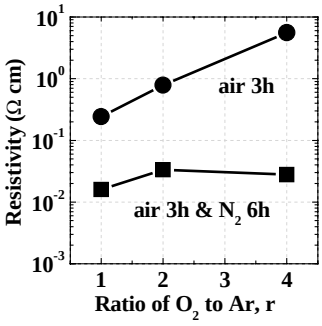

Fig. 9. Resistivity of samples prepared at atmospheric pressure vs. ratio (r) of O_2 to Ar.

a reference. Transmittance of the untreated PG50 at 550 nm is about 33%. The low transmittance is ascribed to a strong Rayleigh scattering of light by its pores. The scattering appears very strong especially in UV-Vis region. This can be verified from the spectra measured with IS. The transmittance of the ITO/PG nanocomposite is only 0.8% without IS, and up to 32% measured with IS, at 550 nm. If back-scattered light is also accounted, the measured transmittance should increase more. In fact, the nanocomposite looks like not opaque at all, but translucent due to the scattering.

When the nanocomposite is used as an electrode in a photoelectric device, the functional materials anchored in the pores may effectively utilize this scattered light. Iida et al. [17] have indicated that a milky SnO_2 film which consisted of large particles, showed higher light-to-energy conversion efficiency than that of a transparent film, when used as an electrode in an a-Si solar cell. This is because the large particles form a texture on the interface with silicon, which decrease optical reflection and enhance confinement of incident light.

Surface area versus pore diameter of ITO/PG nanocomposite when $r = 4$, is shown in Fig. 8. Comparing with an untreated PG50, the ITO/PG nanocomposite shows a peak shift to small pore diameter side, means that the pores certainly remain after growth of ITO particles and their diameter becomes smaller than that of PG50. This is in agreement with FESEM observation. It also shows an increase of specific surface area from 55 to 79 m^2/g, which is ascribed to the fine structure of the ITO particles, since the increase of surface area is almost shown in pores with pore diameter less than 10 nm. A surface area per unit area can be calculated by multiplying the measured specific surface area by weight of the sample and dividing it by the area of one side of the sample. It gives $A \times W/S = (79\,m^2/g)(0.17\,g/1.767\,cm^2) = 7.6\,m^2/cm^2$, where A is the specific surface area measured, W the measured weight of the sample, and S is the top area of the sample plate. On the other hand, for a plane TCF without considering its roughness, the above number should be $1\,cm^2/cm^2$. Therefore, the surface area per unit area for the nanocomposite is about 7.6×10^4 times larger than that of a plane TCF.

3.2. ITO film prepared on PG50 at atmospheric pressure (see Fig. 2)

Samples prepared at atmospheric pressure give similar XRD patterns as those prepared by evacuating from one side of PG50. Fig. 9 shows resistivity of the obtained samples versus the ratio (r) of O_2 to Ar. The resistivity is about $2–3 \times 10^{-2}\,\Omega\,cm$, which is 10 times lower than that of the ITO/PG nanocomposites stated above. Moreover, the transmittances of the samples are higher than that of the ITO/PG nanocomposites above. A typical SEM image of the sample prepared at atmospheric pressure when $r = 2$, is shown in Fig. 10. Comparing to the image of ITO/PG nanocomposite shown in Fig. 5, it can be seen that the sample prepared

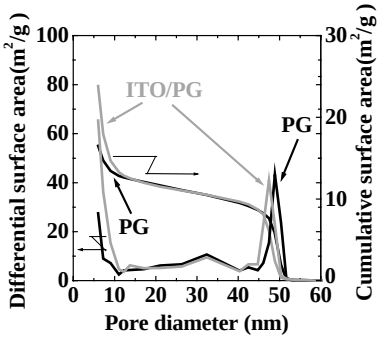

Fig. 8. Surface area vs. pore diameter of sample prepared by evacuating from one side of PG50 when $r = 4$, and an untreated PG50 for reference.

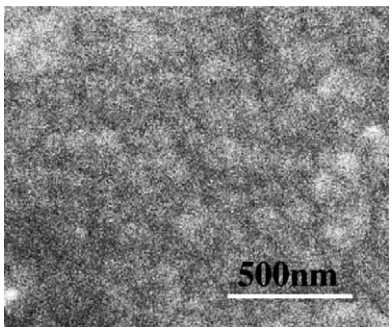

Fig. 10. SEM surface image of sample prepared at atmospheric pressure when $r = 2$. Bar: 500 nm.

at atmospheric pressure is flat, and is formed by small and densely packed particles. Therefore, it showed lower resistivity and higher transmittance than the ITO/PG nanocomposite with porous structure.

Generally it is difficult to prepare film on PG uniformly [14] and/or with a low resistivity [15]. According to [14], an ITO film prepared on PG with pore diameter of 10 nm, has thickness of ∼3 μm and sheet resistance of 1.0 kΩ/□, that is, resistivity of $3 \times 10^{-1}\,\Omega\,\text{cm}$. In the present study, ITO film is prepared on PG with larger pore diameter of 50 nm, and it has lower resistivity of $2–3 \times 10^{-2}\,\Omega\,\square$,. Thus, the present ITO film on PG is sufficient for many practical applications in photoelectric devices. Moreover, the preparation method at atmospheric pressure can also be used when the pore of the ITO/PG nanocomposite need to be sealed with a flat, dense conductive film. For example, when the ITO/PG nanocomposite is used as an electrode of dye-sensitized solar cell, the pores of the electrode need to be sealed because liquid electrolyte will be in the pores.

4. Summary

Translucent conductive porous ITO/PG nanocomposite is obtained by introducing conductive ITO into the pores of a porous matrix by MOCVD method with evacuation from one side of the porous matrix. On the other hand, conductive, uniform and dense ITO film on PG plate is obtained at atmospheric pressure. The resistivity of the obtained samples is about 10^{-1} to $10^{-2}\,\Omega\,\text{cm}$. The transmittance is more than 30% at 550 nm without considering back-scattered light. The obtained ITO/PG nanocomposite has through pores, and a large surface area of $79\,\text{m}^2/\text{g}$, which is about 7.6×10^4 times larger than that of a plane TCF.

References

[1] B. O'Regan, M. Gratzel, Nature 353 (24) (1991) 737–739.
[2] C.J. Barbe, F. Arendse, P. Comte, M. Jirousek, F. Lenzmann, V. Shkjover, M. Gratzel, J. Am. Ceram. Soc. 80 (12) (1997) 3157–3171.
[3] H. Lin, T. Yoko, M. Takahashi, Japanese Patent, Open No. 2001-44469 (1999).
[4] O.O. Akinwunmi, M.A. Eleruja, J.O. Olowolafe, G.A. Adegboyega, E.O.B. Ajayi, Opt. Mater. 13 (1999) 255–259.
[5] Y. Sawada, C. Kobayashi, S. Seki, H. Funakubo, Thin Solid Films 409 (2002) 46–50.
[6] T. Karasawa, Y. Miyata, Thin Solid Films 233 (1993) 135.
[7] C. Liu, T. Matsutani, N. Yamamotoand, M. Kiuchi, Europhys. Lett. 59 (4) (2002) 606–611.
[8] M.E. Nordberg, J. Am. Ceram. Soc. 27 (10) (1944) 299–305.
[9] A.J.G. Zarbin, M.D. Vargas, O.L. Alves, J. Mater. Chem. 9 (1999) 519–523.
[10] A.J.G. Zarbin, M.D. Paoli, O.L. Alves, Synth. Met. 99 (1999) 227–235.
[11] S. Nakagaki, A.R. Ramos, F.L. Benedito, P.G. Peralta-Zamora, A.J.G. Zarbin, J. Mol. Catal. A: Chem. 185 (2002) 203–210.
[12] H. Yamashita, Y. Ichihashi, M. Harada, G. Stewart, M.A. Fox, M. Anpo, J. Catal. 158 (1996) 97–101.
[13] S.Z. Chu, S. Inoue, K. Wada, D. Li, H. Haneda, J. Mater. Chem. 868 (2003) 866–870.
[14] J. Dong, H.D. Gafney, J. Non-Cryst. Solids 203 (1996) 329–333.
[15] H. Lin, T. Jin, A. Dmytruk, T. Yazawa, J. Cerem. Soc. Jpn. 112 (4) (2004).
[16] H. Kimura, H. Watanabe, T. Ishihara, Y. Suzuki, K. Ito, Jpn. J. Appl. Phys. 30 (6) (1987) C546–C554.
[17] H. Iida, N. Shiba, T. Mishuku, H. Karasawa, A. Ito, M. Yamanaka, Y. Hayashi, IEEE Elec. Dev. Lett. 4 (5) (1983) 157–159.